Engineering Fracture Mechanics Vol. 16, No. 5, pp. 683–693, 1982
Printed in Great Britain.

0013-7944/82/050683-11$03.00/0
Pergamon Press Ltd.

ON CRACK–CRACK INTERACTION AND COALESCENCE IN FATIGUE

ROGER CHANG
Rockwell International Science Center, Thousand Oaks, CA 91360, U.S.A.

Abstract—The effect of crack–crack interaction and coalescence in fatigue was studied for a single pair of cracks analytically and for multi-cracks based on real microstructure variations by means of Monte Carlo simulations. Crack–crack interaction and coalescence lower the mean fatigue lifetime. The magnitude of lowering increases with increasing crack density and becomes particularly important in the low failure probability regime. Results of this investigation provide insight for laying the foundation of quantitative predictive technology on crack interaction and coalescence aspects of fatigue.

INTRODUCTION

CRACK–CRACK interaction, leading to accelerated growth and coalescence, is a timely subject in nondestructive fatigue life prediction of structural components. Sophisticated nondestructive methods currently under developemnt[1] will permit estimation of the size and shape of cracks and prediction of fatigue lifetime according to conventional fracture mechanics methodology. The predicted lifetime will be shortened, however, if crack–crack interaction and coalescence take place. Although analytical solutions for the interaction of coplanar[2–4] and noncoplanar[5, 6] cracks in two dimensions have been reported in the literature, similar information on crack–crack interaction in three dimensions is absent even for the simplest geometric shapes such as circles and ellipses. There is also very limited information in the literature on the statistical nature of microcrack coalescence, particularly the effect of microstructural variations.

The present investigation is composed of three parts. Part one presents quantitative expressions for the stress-fields and stress intensity factors of a pair of cracks. Part two provides a quantitative estimation of the degradation in crack propagation lifetime due to the interaction and coalescence of a single pair of cracks. Part three describes in detail a Monte Carlo simulation of fatigue, taking into consideration multi-crack coalescence based on real microstructures. It is hoped that the investigation will provide insight toward laying the foundation for quantitative predictive technology on crack interaction and coalescence aspects of fatigue.

QUANTITATIVE EXPRESSIONS FOR STRESS INTENSITY FACTORS

Analytical expressions for stresses, displacements, and stress intensity factors for a single circular/elliptical crack have been reported in the literature[4, 7, 8]. When two cracks coexist, the stress fields in three dimensional space are additive. The full stress field expressions around a circular crack are lengthy and cumbersome. Therefore, we prefer the simpler asymptotic approximation such as that adopted by Benthem and Koiter[3]. The asymptotic approximation is particularly attractive for investigations of crack–crack interaction, since the interaction strength becomes significant only when the two cracks are in close proximity. For two parallel circular cracks of diameters a_1, a_2 and separations l, h, shown schematically in Fig. 1, the normal stresses (to the crack plane) at locations A, B, C, D according to the asymptotic approximation are given by,

$$S_A = \frac{k_1}{\sqrt{(2\epsilon)}} + \frac{k_2}{4\sqrt{(2\Omega_{AC})}}\left(5\cos\frac{\theta_A}{2} - \cos\frac{5\theta_A}{2}\right) \tag{1a}$$

$$S_B = \frac{k_1}{\sqrt{(2\epsilon)}} + \frac{k_2}{4\sqrt{(2\Omega_{BC})}}\left(5\cos\frac{\theta_B}{2} - \cos\frac{5\theta_B}{2}\right) \tag{1b}$$

$$S_C = \frac{k_2}{\sqrt{(2\epsilon)}} + \frac{k_1}{\sqrt{(2\Omega_{CB})}}\left(5\cos\frac{\theta_c}{2} - \cos\frac{5\theta_C}{2}\right) \tag{1c}$$

$$S_D = \frac{k_2}{\sqrt{(2\epsilon)}} + \frac{k_1}{4\sqrt{(2\Omega_{DB})}}\left(5\cos\frac{\theta_D}{2} - \cos\frac{5\theta_D}{2}\right) \tag{1d}$$

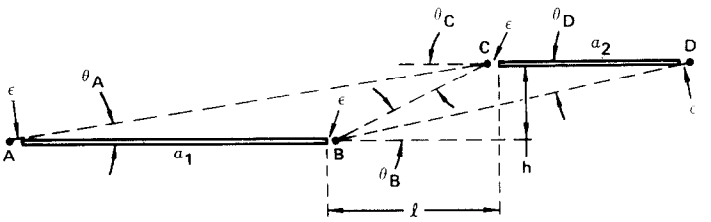

Fig. 1. Sectional view of two parallel circular cracks of radii a_1, a_2 and separations l, h.

where

$$\begin{aligned}
&\Omega_{AC} = \sqrt{x_A^2 + h^2}, \cos\theta_A = x_A/\Omega_{AC}, && x_A = a_1 + l + \epsilon \\
&\Omega_{BC} = \sqrt{x_B^2 + h^2}, \cos\theta_B = x_B/\Omega_{BC}, && x_B = l - \epsilon \\
&\Omega_{CB} = \sqrt{x_c^2 + h^2}, \cos\theta_C = x_c/\Omega_{CB}, && x_C = l - \epsilon \\
&\Omega_{DB} = \sqrt{x_D^2 + h^2}, \cos\theta_D = x_D/\Omega_{DB}, && x_D = a_2 + l + \epsilon.
\end{aligned} \tag{1e}$$

The first term on the r.h.s. of eqns (1a–1d) is the normal stress associated with the crack itself. The second term corresponds to an additional normal stress contribution from the neighboring crack. k_1, k_2 are, respectively, the stress intensity factors for the individual circular cracks of diameters a_1, a_2. The stress singularity parameter, ϵ, is arbitrarily chosen so that the interacting stress fields at locations A, B, C, D are given by the set of eqns (1a–1d). Equations (1b, 1c) are expected to be slightly more rigorous than eqns (1a, 1d), since B, C are in closer proximity to each other than A, D. The stress singularity parameter, ϵ, is much smaller than either a_1 or a_2 and is dependent on both the crack sizes a_1, a_2 and separations l, h. A judicial choice of the dependence of ϵ on a_1, a_2, l, h will tend to partially correct the slight inaccuracies associated with eqns (1a–d).

The stress intensity factors at locations A, B, C, D are calculated according to the stress ratio method previously developed by the author[9]. The respective stress intensity factors, normalized against that of a single circular crack of diameter a_1, are readily obtained according to the stress ratio method by division of eqns (1a–1d) with the common factor $k_1/\sqrt{(2\epsilon)}$,

$$\Delta K_A' = 1.0 + \sqrt{\left(\frac{a_2}{a_1}\right)}\sqrt{\left(\frac{\epsilon}{\Omega_{AC}}\right)}\left(\frac{5}{4}\cos\frac{\theta_A}{2} - \frac{1}{4}\cos\frac{5\theta_A}{2}\right) \tag{2a}$$

$$\Delta K_B' = 1.0 + \sqrt{\left(\frac{a_2}{a_1}\right)}\sqrt{\left(\frac{\epsilon}{\Omega_{BC}}\right)}\left(\frac{5}{4}\cos\frac{\theta_B}{2} - \frac{1}{4}\cos\frac{5\theta_B}{2}\right) \tag{2b}$$

$$\Delta K_C' = \sqrt{\left(\frac{a_2}{a_1}\right)} + \sqrt{\left(\frac{\epsilon}{\Omega_{CB}}\right)}\left(\frac{5}{4}\cos\frac{\theta_C}{2} - \frac{1}{4}\cos\frac{5\theta_C}{2}\right) \tag{2c}$$

$$\Delta K_D' = \sqrt{\left(\frac{a_2}{a_1}\right)} + \sqrt{\left(\frac{\epsilon}{\Omega_{DB}}\right)}\left(\frac{5}{4}\cos\frac{\theta_D}{2} - \frac{1}{4}\cos\frac{5\theta_D}{2}\right). \tag{2d}$$

Equations (2a–2d) have the common feature that, at large crack–crack separations, the stress intensity factors are reduced to those of the individual cracks. A second feature of the asymptotic approximation is that the stress field and stress intensity factor expressions for cracks in two dimensional and three dimensional space are similar, except for the trigonometric terms on the far r.h.s. of eqns (1a–d) and (2a–d). This makes possible the evaluation of the stress singularity parameter ϵ from two dimensional crack–crack interaction whose analytical expressions are available in the literature.

The exact functional dependence of the stress singularity parameter ϵ on a_1, a_2, l, h is not known. We resort, in the present investigation, to an empirical evaluation of this dependence. We assume that ϵ is only weakly dependent on the separation distance h for small h, and that the dependence of ϵ on h is

ignored. After considerable deliberation, we propose the following empirical expression† relating ϵ to a_1, a_2, l,

$$\epsilon = 0.056\left(\frac{a_2}{a_1}\right)^{1/3}\exp\left(-3.11\sqrt{(l/a_2)}\right). \tag{3}$$

In future investigations, the weak dependence of ϵ on h can be incorporated into eqn (3), if necessary. As mentioned before, the similarity in the stress intensity factor expressions between two- and three-dimensional systems makes possible the empirical evaluation of the dependence of ϵ on a_1, a_2, l, h from two-dimensional crack–crack interaction studies. The stress intensity factor expressions for two-dimensional parallel cracks of width a_1, a_2 and separations l, h (schematic diagram same as Fig. 1) according to the asymptotic approximation are,

$$\Delta K_A'' = 1.0 + \sqrt{\left(\frac{a_2}{a_1}\right)}\sqrt{\left(\frac{\epsilon}{\Omega_{AC}}\right)}\cos\frac{\theta_A}{2}\left(1+\sin\frac{\theta_A}{2}\sin\frac{3\theta_A}{2}\right) \tag{4a}$$

$$\Delta K_B'' = 1.0 + \sqrt{\left(\frac{a_2}{a_1}\right)}\sqrt{\left(\frac{\epsilon}{\Omega_{BC}}\right)}\cos\frac{\theta_B}{2}\left(1+\sin\frac{\theta_B}{2}\sin\frac{3\theta_B}{2}\right) \tag{4b}$$

$$\Delta K_C'' = \sqrt{\left(\frac{a_2}{a_1}\right)} + \sqrt{\left(\frac{\epsilon}{\Omega_{CB}}\right)}\cos\frac{\theta_C}{2}\left(1+\sin\frac{\theta_C}{2}\sin\frac{3\theta_C}{2}\right) \tag{4c}$$

$$\Delta K_D'' = \sqrt{\left(\frac{a_2}{a_1}\right)} + \sqrt{\left(\frac{\epsilon}{\Omega_{DB}}\right)}\cos\frac{\theta_D}{2}\left(1+\sin\frac{\theta_D}{2}\sin\frac{3\theta_D}{2}\right) \tag{4d}$$

where the Ω parameters and trigonometric functions are as defined in eqn (1e).

Analytical expressions for the stress intensity factors for a pair of parallel and coplanar ($h = 0$) two dimensional cracks of widths a_1, a_2 and separation l from the literature [10] are,

$$\Delta K_A = \sqrt{\left(1+\frac{a_2}{a_1}+\frac{l}{a_1}\right)\left(1+\frac{l}{a_1}\right)}\left[1-\frac{a_2+l}{a_1+a_2+l}\frac{E(k)}{K(k)}\right] \tag{5a}$$

$$\Delta K_B = \sqrt{\left(\frac{l}{a_2}\left(1+\frac{l}{a_2}\right)\right)}\left[\frac{a_2(a_1+l)}{a_1 l}\frac{E(k)}{K(k)}-\frac{a_2}{a_1}\right] \tag{5b}$$

$$\Delta K_C = \sqrt{\left(\frac{l}{a_2}\left(1+\frac{l}{a_1}\right)\right)}\left[\frac{a_2+l}{l}\frac{E(k)}{K(k)}-1\right] \tag{5c}$$

$$\Delta K_D = \sqrt{\left(1+\frac{a_2}{a_1}+\frac{l}{a_1}\right)\left(1+\frac{l}{a_2}\right)}\left[1-\frac{a_1+l}{a_1+a_2+l}\frac{E(k)}{K(k)}\right] \tag{5d}$$

where $E(k)$, $K(k)$ are, respectively, complete elliptical integrals of the second kind and first kind, and $k = \sqrt{((a_1a_2/(a_1+l)(a_2+l))}$. Comparisons of the $\Delta K''$ values calculated according to eqns (4a–d) proposed in this investigation and the ΔK values according to eqns (5a–d) from the literature [10] are shown in Fig. 2 for l/a_2 varying between 0.1 and 2.0, and a_2/a_1 varying between 0.5 and 1.0. The agreement between the two sets of calculations is excellent, suggesting that the empirical expression relating ϵ to a_1 a_2, l given by eqn (3) is satisfactory.

The stress intensity factors for two dimensional parallel noncoplanar cracks ($a_1 = a_2$, $h \neq l \neq 0$) according to a continuously distributed dislocation model have also been reported in the literature [6]. Comparisons of the $\Delta K''$ values calculated according to eqns (4a–d) proposed in this investigation and those obtained numerically in the literature [6] are shown in Fig. 3 for l/a_2 varying between 0.5 and 3.0, h/a_1 varying between 0.01 and 3.0 and $a_1 = a_2$. The agreement between the two sets of calculations is also satisfactory.

†Some guidance as to the formalism of eqn (3) is obtained by equating eqns (4a–d) with eqns (5a–d) to solve ϵ as functions of a_1, a_2, l.

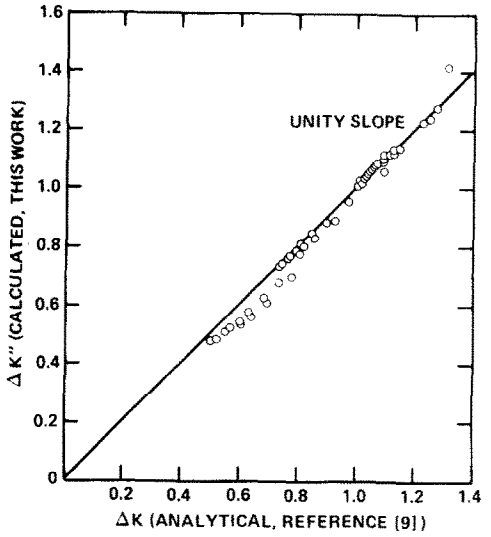

Fig. 2.

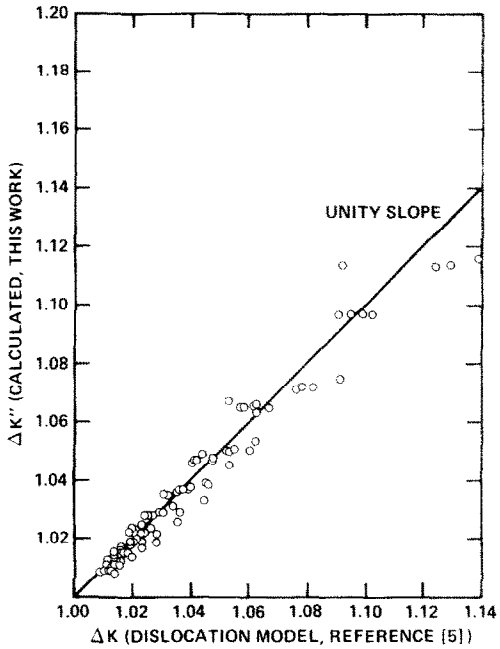

Fig. 3.

Fig. 2. Comparison of stress intensity factors for two interacting parallel coplanar cracks of widths a_1, a_2 and various separations in two-dimensional space calculated according to this work ($\Delta K''$) and those reported in the literature (ΔK).

Fig. 3. Same as Fig. 2, two interacting parallel noncoplanar cracks in two-dimensional space.

QUANTITATIVE ESTIMATION OF FATIGUE CRACK PROPAGATION LIFETIME DEGRADATION DUE TO CRACK–CRACK INTERACTION

In this section the lowering of fatigue crack propagation lifetime due to crack–crack interaction will be estimated. First we calculate the equivalent circular crack radius corresponding to a pair of circular cracks of given size and separation which coalesce after touching but do not interact prior to coalescence. We then calculate the equivalent circular crack radius for the same pair of cracks which interact according to eqns (2a–d) prior to touching and coalescence. The difference in equivalent circular crack radius for the two cases yields directly the fatigue lifetime lowering due to crack–crack interaction. Only parallel coplanar circular cracks are treated in this investigation, however.

The growth rate of an individual circular crack of radius R can be described by the following expression,

$$\frac{dR}{dN} = a\Delta K^{\alpha} \tag{6}$$

where N is the fatigue cycles; "a" is a material constant; ΔK is the applied Mode I stress intensity range; α is the Paris crack growth exponent (usually varying between 2 and 4). The stress intensity range under a given applied normal stress range ΔS is given by,

$$\Delta K = \frac{2}{\pi}\Delta S\sqrt{(\pi R)}. \tag{7}$$

Combination of eqns (6) and (7) and integration over the limits R_0 and R yields (R_0 is the initial radius),

$$R^{-(\alpha/2)+1} - R_0^{-(\alpha/2)+1} = \left(-\frac{\alpha}{2}+1\right)bN, \qquad b = \frac{a\Delta S^{\alpha}2^{\alpha}}{\pi^{\alpha/2}}. \tag{8}$$

The equivalent circular crack radius R_e corresponding to a pair of coplanar circular cracks of radii

R_1, R_2 and center to center separation d for equal propagation lifetime is estimated in three consecutive steps as follows:

Step one

The number of fatigue cycles needed for the two coplanar cracks to touch each other in absence of crack–crack interaction is, according to eqn (8),

$$\Delta N = R_x^{-(\alpha/2)+1} - R_2^{-(\alpha/2)+1} = R_{d-x}^{-(\alpha/2)+1} - R_1^{(\alpha/2)+1} \tag{9}$$

where R_x, R_{d-x} are, respectively, the final radii of the second crack (original radius R_2) and the first crack (original radius R_1) after ΔN fatigue cycles. With given inputs of R_1, R_2, d, α, eqn (9) can be readily solved for R_x, R_{d-x} and ΔN.

Step two

On touching, the two cracks are replaced by an equivalent circular crack of radius R_y according to the equivalent area approximation previously proposed by the author[11], based on energy consideration.

Step three

The equivalent circular crack of radius R_y is allowed to shrink uniformly in the same time frame of ΔN fatigue cycles to yield R_e according to the following expression

$$R_y^{-(\alpha/2)+1} - R_e^{-(\alpha/2)+1} = \Delta N. \tag{10}$$

In the presence of crack–crack interaction, eqn (9) no longer holds. ΔN in step one must be evaluated numerically in small fatigue increments $\Delta n (\Delta n \ll \Delta N)$ according to the crack growth eqn (6) and the stress intensity factor eqns (2a–d) until the two cracks touch. The same steps two and three are then used to obtain R_e. The results of one set of calculations for $a_1 = a_2$, $\alpha = 3.5$ and various d values are summarized in Table 1 and plotted in Fig. 4. There should be no change in equivalent circular crack radius R_e at zero crack–crack separation. The percent increase in R_e (or decrease in fatigue crack propagation lifetime) rises rapidly with increasing crack–crack separation, reaches a maximum, then falls gradually to zero at infinite crack–crack separation.

MONTE CARLO SIMULATION

There is very limited information in the literature on the statistical nature of microcrack coalescence. Lindberg[12] and McClintock[13] approached the problem by means of simple statistical methods. Hunt[14] solved the statistical linking of microcracks exactly in one-dimension and presented approximate solutions for two- and three-dimensions for low crack densities which become exact in the continuum limit and reduce to a generalization of Weibull's statistical theory of failure and classical reliability theory. These treatments are grossly simple. The details of crack nucleation and growth from the microstructural point of view have been ignored. We attempt to approach the statistical behavior of microcrack coalescence taking into consideration the effect of microstructure variations, principally the

Table 1. Equivalent circular crack radius (R_e) calculation corresponding to two parallel coplanar circular cracks of same radius (R_1) and various separations with and without crack–crack interaction

Center to Center Separation (units of R_1)	R_e(No Interaction) (units of R_1)	R_e(Interaction) (units of R_1)	Percent Difference
2.5	1.314	1.372	4.4
3.0	1.265	1.360	7.5
4.5	1.184	1.272	7.4
6.0	1.158	1.221	5.4
12.0	1.082	1.107	2.3
18.0	1.059	1.072	1.2
26.0	1.044	1.052	0.8

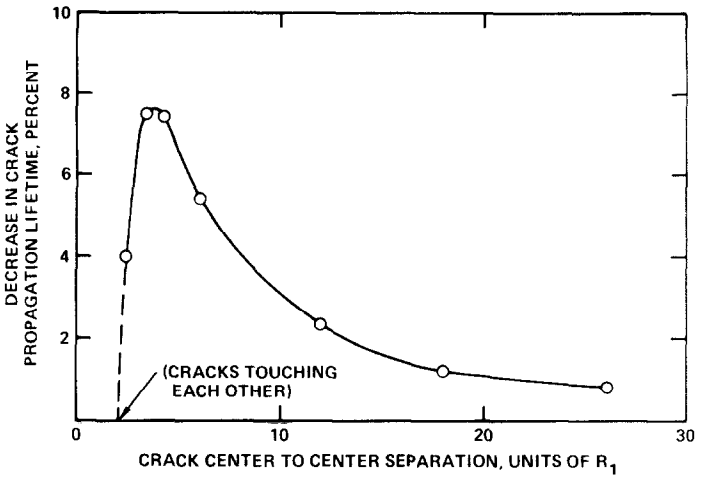

Fig. 4. Degradation of fatigue crack propagation lifetime as function of separation distance for a pair of parallel coplanar circular cracks of equal radius in three-dimensional space.

grain size and inclusion distributions, on the kinetics of crack nucleation, growth and coalescence by means of Monte Carlo simulations.

Details of our Monte Carlo approach to microcrack nucleation and growth have appeared elsewhere[15, 16] and will not be elaborated further. The methodology employed in this investigation differs somewhat from that used in Ref. [16]. The computational procedures are as follows:

(1) Generate random microstructures according to experimental grain size and inclusion distributions for the material under study.

(2) Compute crack initiation time for each of the inclusions at a given applied cyclic stress according to the crack initiation expressions given in Ref. [15] and employing a predetermined set of modeling constants. (The modeling constants were chosen to fit experimental crack initiation data.)

(3) Begin crack growth calculation at incremental time intervals for those cracks which have been initiated according to the crack growth expressions given in Ref. [16] and employing again a selected set of modeling constants. New cracks will be initiated from time to time and their growth followed.

(4) Check for possible crack coalescence and print out at each incremental time interval and size and location of all cracks.

(5) Set a critical crack size for catastrophic failure. Continue calculation if the maximum crack size is less than the critical value. Otherwise terminate calculation and plot out the crack distribution just prior to catastrophic failure.

We attempted initially to incorporate the full crack–crack interaction and coalescence methodology described in the preceding section into the Monte Carlo simulation in Step 4. Since this is too time consuming and costly, a simplified procedure was adopted: two parallel cracks, coplanar or otherwise, are allowed to coalesce when their closest distance of approach falls within 7% of their total cross sectional width. This number is in accordance with the crack–crack interaction calculations given in the preceding section. The capture cross section for crack–crack coalescence is assumed to be of the order of the maximum decrease in crack propagation lifetime (see Table 1 and Fig. 4) due to crack–crack interaction. This capture cross section is also in agreement with experimental observations from our laboratory[17]. The simplified procedure saves considerable computer time and is not believed to affect the simulation results very much.

A total of about 2000 simulation runs were made. The statistical grain size and inclusion distributions for an aluminum 2219T851 alloy containing 100 inclusions/cm^2 and 400 inclusions/cm^2 were used as inputs. The simulation was done at three maximum cyclic stress levels, corresponding to 60, 75 and 90% of the yield stress of the material. The simulation is two dimensional, representing the surface or a planar cross section of the interior. The critical crack length was arbitrarily chosen to be 1500 microns.

A typical computer plot of crack distribution at the end of a simulation run is reproduced in Fig. 5. It is to be noted from Fig. 5 that not all nucleated cracks grow. This is distinctly a microstructural effect which could not be predicted by any conventional fracture mechanics and/or statistical treatments. Typical cumulative distributions of crack sizes at various states of fatigue life for a given simulation run

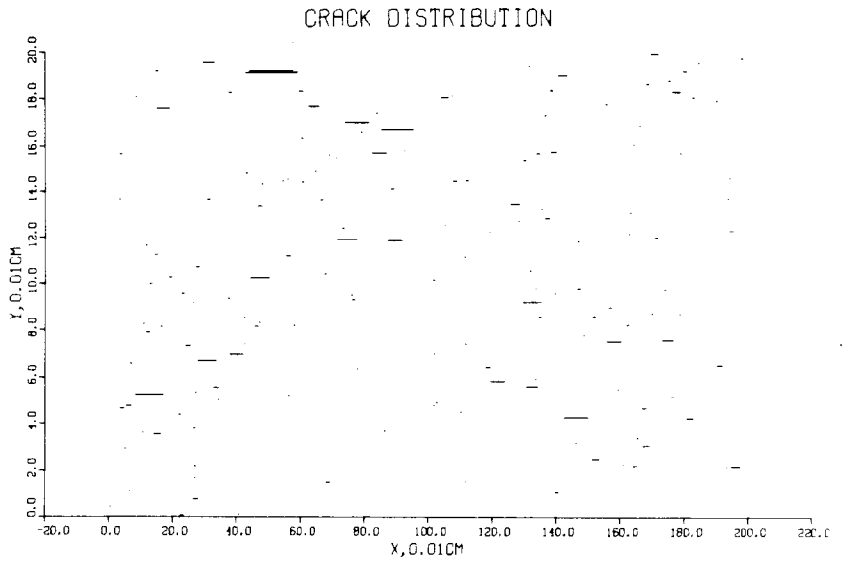

Fig. 5. Typical computer plot of crack distribution at the end of a Monte Carlo simulation run (double line at upper left of figure indicating a coalesced crack of order $N = 2$).

are shown in Fig. 6; the plots of many independent simulation runs for a given inclusion density are quite similar and are not presented here for the sake of space.

The number of coalesced cracks of size N($N = 2$ for 2-crack coalescence, $N = 3$ for 3-crack coalescence, etc.) was counted for every simulation run. The fraction of coalesced cracks of size N was plotted vs N, in Figs. 7 and 8, for the two inclusion densities (100/cm^2 and 400/cm^2); each plot represented about 1000 simulation runs.

A typical frequency plot of fatigue lifetimes for simulation runs obtained at 75% yield stress and 100 inclusions/cm^2 is shown in Fig. 9. There are six such plots covering, respectively, three applied cyclic stress levels and two inclusion densities, but only one is shown here. The mean fatigue lifetime for the six series of runs with and without coalescence are summarized in Table 2.

The cumulative distribution of fatigue lifetimes for all the simulation runs are plotted in Figs. 10–12 for, respectively, the three applied cyclic stress levels; each figure is composed of four curves comparing the two inclusion densities and coalescence/no coalescence effects. The fatigue lifetime results obtained in this investigation will be slightly underestimated as the incubation time for a crack to cross a grain boundary[19] is ignored. The neglect of this incubation time is not expected to alter the general trends presented here, however.

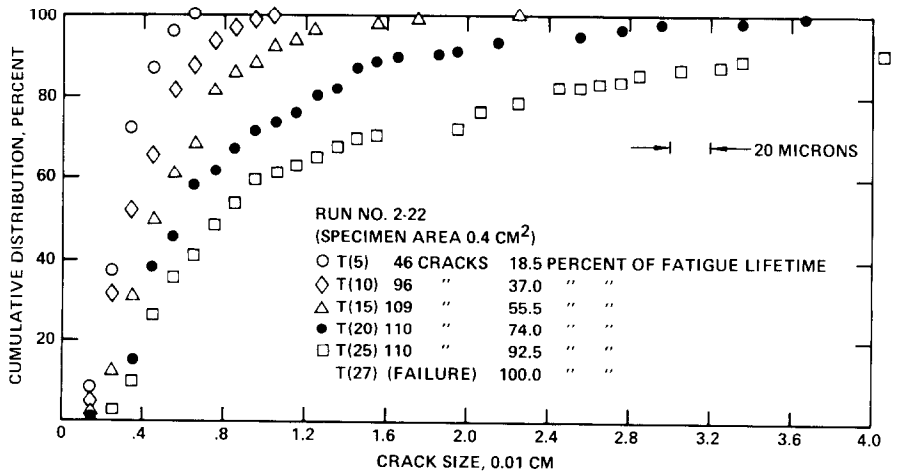

Fig. 6. Typical cumulative distribution of crack sizes at various stages of fatigue life during a simulation run.

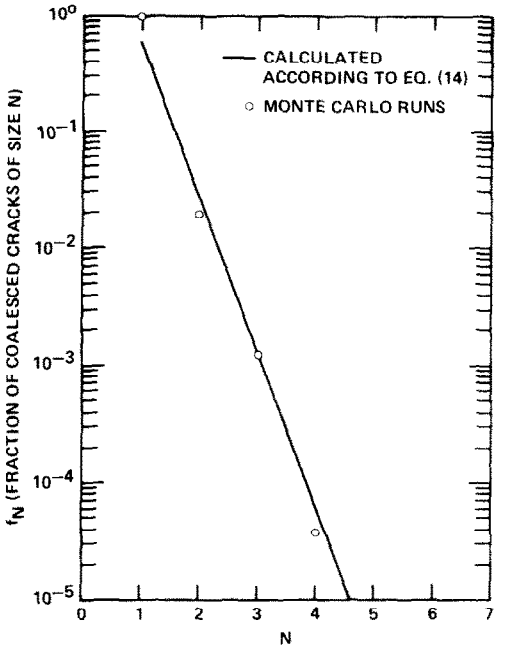

Fig. 7.

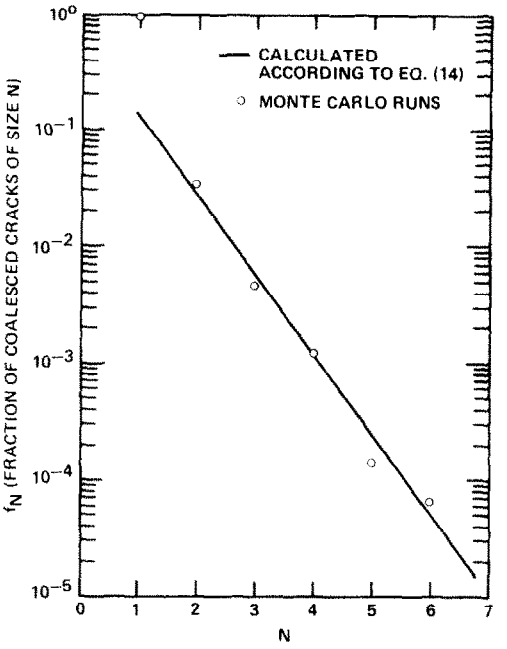

Fig. 8.

Fig. 7. Semilogarithmic plot of fraction of cracks of size N vs N (100 inclusions/cm^2).
Fig. 8. Semilogarithmic plot of fraction of cracks of size N vs N (400 inclusions/cm^2).

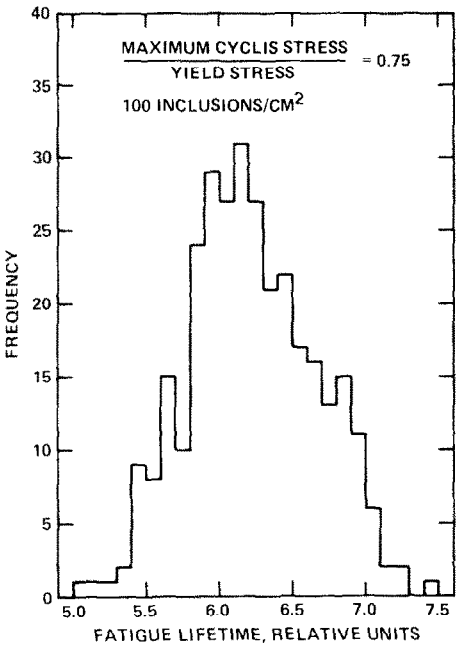

Fig. 9. Frequency distribution of fatigue lifetime for aluminum 2219T851 alloy containing 100 inclusions/cm^2 and fatigued under maximum cyclic stress at 75% of yield stress.

Table 2. Mean fatigue lifetime from six series of runs (3 applied cyclic stress levels and 2 inclusion densities) with and without coalescence

Applied Cyclic Stress (Per Cent of Yield Stress)	Inclusion Density (number/cm^2)	Mean Fatigue Lifetime (Relative Units) Coalescence	No. Coalescence
60	100	9.616 ± 0.678	9.655 ± 0.643
75	100	6.223 ± 0.431	6.248 ± 0.434
90	100	4.340 ± 0.295	4.371 ± 0.292
60	400	8.741 ± 0.428	8.903 ± 0.413
75	400	5.622 ± 0.300	5.734 ± 0.263
90	400	3.942 ± 0.214	4.007 ± 0.191

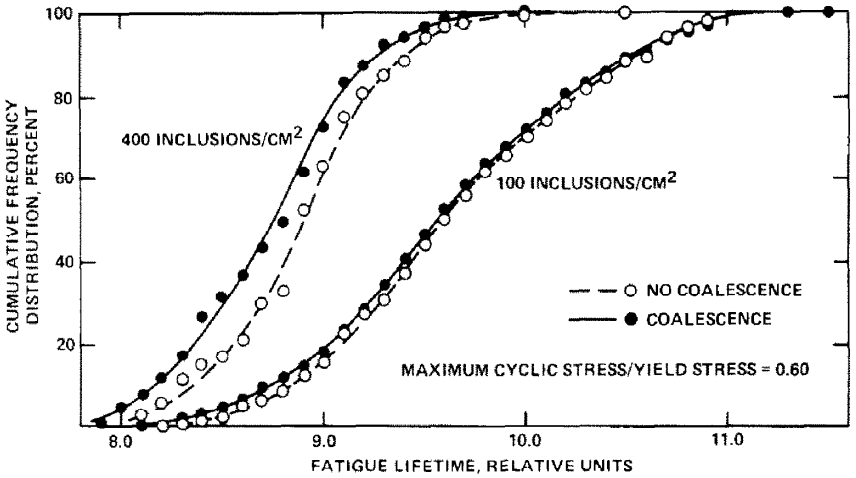

Fig. 10. Cumulative distribution of fatigue lifetime comparing effect of inclusion density and of coalescence, fatigued at 60% of yield stress.

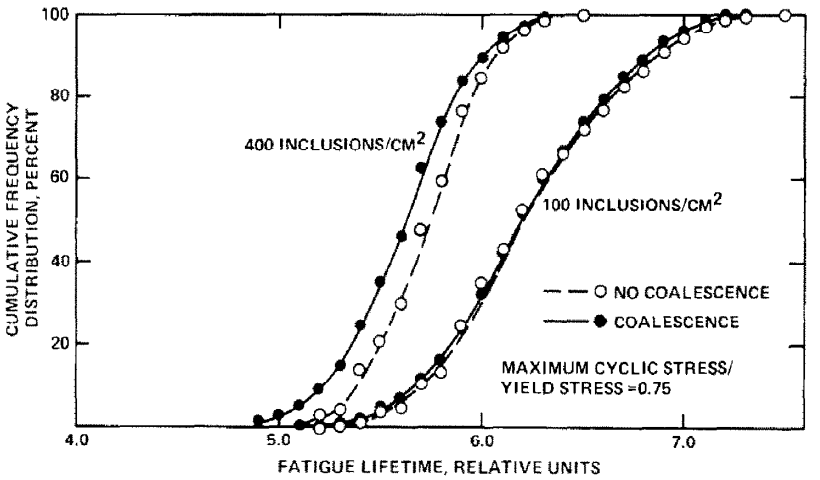

Fig. 11. Same as Fig. 10, fatigued at 75% of yield stress.

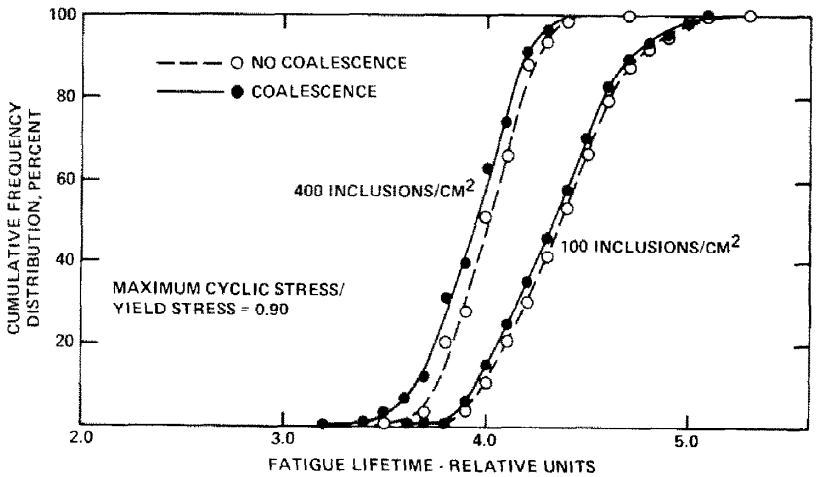

Fig. 12. Same as Fig. 10, fatigued at 90% of yield stress.

DISCUSSION

The cumulative crack size distributions at various stages of fatigue life, shown typically in Fig. 6, are quite reproducible from simulation run to simulation run. This points to the possibility that the crack size distribution characteristics may be used to estimate the remaining mean fatigue lifetime of structural components, particularly if quantitative nondestructive means to evaluate crack size distribution is available experimentally. This should be an interesting field for more elaborate investigation.

The probability of finding coalesced cracks of size N, shown in Figs. 7 and 8, varies exponentially with N. The exact statistical distribution functions of extreme values have been discussed in the literature[18]. We conclude that the probability distribution function of coalesced cracks of size N from our Monte Carlo simulation runs follows the exponential type. We thus write the following cumulative distribution function for coalesced cracks of size N[18],

$$F(N) = 1 - \frac{1}{\rho} \exp\{-\alpha_\rho[(N-1)L - U_\rho]\} \tag{11}$$

where ρ is the inclusion density; L is the mean distance between inclusions; α_ρ and U_ρ are material constants which may be dependent on ρ. Differentiation of eqn (11) with respect to N yields the probability of finding coalesced cracks of size N,

$$f(N) = \frac{\partial F(N)}{\partial N} = \frac{\alpha_\rho}{\rho} \exp\{-\alpha_\rho[(N-1)L - U_\rho]\}. \tag{12}$$

The number of coalesced cracks of size N is simply the product of ρ and $f(N)$,

$$n(N) = \rho \cdot f(N) = \alpha_\rho \exp\{-\alpha_\rho[(N-1)L - U_\rho]\}. \tag{13}$$

By folding α_ρ into the exponential and replacing L by $\rho^{-1/2}$, eqn (13) becomes,

$$n(N) = \exp\left\{-\frac{a(N-1)}{\sqrt{\rho}} + b\right\} \tag{14}$$

where a and b are material constants. Equation (14) fits both Figs. 7 and 8 with $a = 31.4$, $b = 3.4$, for $\rho = 100/\text{cm}^2$ (Fig. 7) and $\rho = 400/\text{cm}^2$ (Fig. 8). It is to be noted that Figs. 7 and 8 were constructed for a critical crack size of 1500 microns. The constant b in eqn (14) will be smaller (larger) than 3.4 if the critical crack size is smaller (larger) than 1500 microns. Furthermore, it is possible that both a and n could be affected by the details of microstructural variations and the choice of modeling constants used in the Monte Carlo simulation studies. These areas remain subjects for future investigations.

A rather surprising result of the Monte Carlo simulation study is that consideration of crack–crack interaction and coalescence lowers only moderately the mean fatigue lifetime. It is not expected that the general trend will become very different for other choices of the modeling constants than those used in the present investigation.

As engineering structures are designed to sustain long service life, it is usually the regime of low failure probabilities which is most important in fatigue lifetime prediction. Experimentation in this regime can be extremely time consuming and costly and must rely heavily on theoretical predictions. The effect of crack–crack interaction and coalescence becomes increasingly more important in the regime of lower failure probability. This is clearly seen in Figs. 10–12, where the effect of coalescence becomes very important on the low failure probability (far left) side of the plots. Extrapolation of the results shown at the l.h.s. of Fig. 11, e.g. to lower failure probabilities shows that the losses in the fatigue lifetime are 10, 20 and 50% for failure probabilities of 10^{-4}, 5×10^{-7} and 10^{-10}, respectively. The importance of crack–crack interaction and coalescence to fatigue life prediction in the low failure probability regime cannot be over emphasized. Detailed studies in this low failure probability region are currently going on in our laboratory[20].

Acknowledgements—This research was sponsored in part by Rockwell International Independent Research and Development Funds and in part by Contract F33615-80-C-5004 sponsored jointly by the Defense Advanced Research Projects Agency and the Air Force Wright Aeronautical Laboratories.

REFERENCES

[1] See, e.g. *Proc. ARPA/AFML Rev. of Progress in Quantitative NDE, AFML-TR-78-205, AFML-TR-79-*. Rockwell International Science Center.

[2] T. Yokobori and M. Ichikawa, Fracture of crystalline solids with an infinite row of colinear cracks as a result of plastic flow. *Int. J. Fracture* **1**, 217–223 (1965).

[3] J. P. Benthem and W. T. Koiter, Asymptotic approximations to crack problems. *Mechanics of Fracture I, Methods of Analysis and Solutions of Crack Problems* (Edited by G. C. Sih), pp. 131–178. Noordhoff (1973).

[4] I. N. Sneddon, Integral transformation methods. *Mechanics of Fracture I, Methods of Analysis and Solutions of Crack Problems* (Edited by G. C. Sih), pp. 314–367. Noordhoff (1973).

[5] M. Isida, Method of Laurent series expansion for internal crack problems. *Mechanics of Fracture I, Methods of Analysis and Solutions of Crack Problems* (Edited by G. C. Sih), pp. 56–130. Noordhoff (1973).

[6] T. Yokobori, M. Uozumi and M. Ichikawa, Interaction between noncoplanar parallel staggered elastic cracks. *Rep. Res. Instit. Strength and Fracture of Materials, Tohoku University, (Japan)* **7**, 25–47 (1971).

[7] G. C. Sih and H. Liebowitz, Mathematical theories of brittle fracture. *Mathematical Fundamentals* (Edited by H. Liebowitz), Vol. II, pp. 68–188. Academic Press, New York (1968).

[8] L. M. Keer, S. Nemat-Nasser and A. Oranratnachai, Spontaneous growth of interacting cracks in a cruciform pattern. *Engng Fracture Mech.* **13**, 15–29 (1980).

[9] R. Chang, Static finite element stress intensity factors for annular cracks. *Rockwell Int. Sci. Center Techn. Rep., SC-PP-80-50.*

[10] T. Matake and Y. Imai, Pop-in behavior induced by interaction of cracks. *Engng Fracture Mech.* **9**, 17–24 (1977).

[11] R. Chang, Fracture mechanics of two-dimensional noncircular flaws—The equivalent area approximation. *Engng Fracture Mech.* **16**, 675–681 (1982).

[12] U. Lindberg, A statistical model for the linking of microcracks. *Acta Metallurgica* **17**, 521–526 (1969).

[13] F. A. McClintock, Statistics of brittle fracture. *Fracture Mechanics of Ceramics*, Vol. 1, *Concepts, Flaws and Fractography* (Edited by R. C. Bradt, D. P. H. Hasselman and F. F. Lange), pp. 93–114. Plenum Press, New York (1973).

[14] R. A. Hunt, A theory of the statistical linking of microcracks consistent with classical reliability theory. *Acta Metallurgica* **26**, 1443–1452 (1978).

[15] R. Chang, W. L. Morris and O. Buck, Fatigue crack nucleation at intermetallic particles in alloys—a dislocation pile-up model. *Scripta Metallurgica* **13**, 191–194 (1979).

[16] W. L. Morris, M. R. James and O. Buck, Computer simulation of fatigue crack initiation. *Engng Fracture Mech.* **13**, 213–221 (1980).

[17] W. L. Morris, O. Buck, H. L. Marcus and R. V. Inman, *Rockwell Int. Sci. Center Techn. Rep. SCTR-74-9*, Fatigue crack initiation in aluminum 2219T851 (1974).

[18] E. J. Gumbel, Statistical theory of extreme values and some practical applications. *United States National Bureau of Standards Appl. Mathematics Series* 33 (1954).

[19] W. L. Morris, M. R. James and O. Buck, Growth rate models for short surface cracks in A12219-851. To appear in *AIME Metallurgical Trans.*

[20] W. L. Morris, Paper presented at ARPA/AFML Review of Progress in Quantitative NDE, La Jolla, California, July 1980, manuscript in preparation.

(*Received* 19 *December* 1980; *received for publication* 27 *July* 1981)